A SIMPLE NEURAL-NETWORK ALGORITHM FOR CLASSIFICATION OF LIDAR SIGNALS APPLIED TO FOREST-FIRE DETECTION

Andrei B. Utkin, Alexander Lavrov

INOV - INESC Inovação, Rua Alves Redol, Lisbon, Portugal

Rui Vilar

DEMAT, Instituto Superior Técnico, Technical University of Lisbon, Lisbon, Portugal

Keywords: Perceptron, Lidar, Signal processing, Singular value decomposition, Radial-basis function networks.

Abstract: Detection of smoke plumes using lidar provides many advantages with respect to passive methods of fire surveillance. However, the great sensitivity of the method results in the detection of many spurious signals. Correspondingly, the automatic lidar surveillance must be provided with effective algorithms of separation of the smoke-plume signatures from irrelevant signals. The paper discusses a simple and robust lidar pattern recognition procedure based on the fast extraction of sufficiently pronounced signal peaks and their classification with a perceptron, whose efficiency is enhanced by a fast nonlinear preprocessing. The algorithm is benchmarked against previously developed artificial-intelligence methods of smoke recognition via Relative Operating Characteristic (ROC curve) analysis.

1 INTRODUCTION

Extending the principles of radar to the optical range, lidar (light detection and ranging) presents significant advantages in comparison with passive surveillance methods, in particular a higher sensitivity and low dependency on light and weather conditions. Lidar detectors provide a large range of surveillance, restricted only by the laser-pulse energy and — for distances exceeding ~10 km — by the beam jitter resulted from atmospheric turbulence. Good directionality and precision of distance measurements enable lidar to provide an accurate location of smoke plumes. For efficient early forest-fire detection, the smoke-plume pattern in the lidar signal (peak of the retroreflected power) must be promptly recognized by an adequate automatic procedure despite the presence of additional peaks due to noise and other targets. The present paper details the investigation of one such procedure based on the fast localization of peaks whose amplitude is sufficiently large to correspond to possible smoke-plume signatures. These peaks are subjected to feature extraction and highly nonlinear binarization transformation, which increases the number of signal components. The binarized patterns are then classified with a single-layer perceptron.

Lidar equipment (Fig. 1) consists of a radiation emitter (pulsed laser and beam-formation optics) and a radiation receiver (usually comprising of a light gathering optical train, photodetector and preamplifier). The emitter produces short and intense radiation pulses; a part of this radiation is scattered backwards and collected by the receiver, where its power is converted into an electric signal. The electric signal is amplified and directed to the data-acquisition unit, to be recorded in a digital form as a function of time.
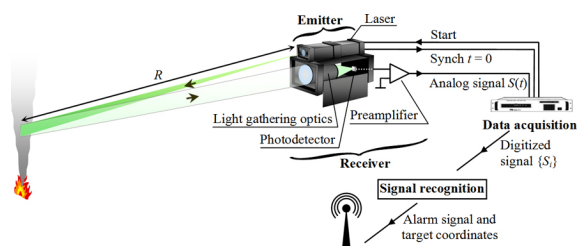

Figure 1: Lidar equipment and detection principles.

Lidars for automated surveillance are supplemented with a signal recognition system, performing classification of target signatures and issuing, if needed, an alarm signal containing information about the target that caused the alarm situation.

2 BASIC RELATIONS

The distance from the lidar to the target R may be calculated from the time delay t between the laser-pulse emission and the reception of the backscattered signal, $t = 2R/c$, c is the velocity of light. The raw lidar signal S is the receiver-unit output voltage recorded during some period of time immediately after the laser-pulse emission ($t = 0$). As far as the transition from the time to the distance dependence is reduced to a simple rescaling, usually the raw lidar signal is represented as a plot of S versus the distance R rather than the time t:

$$S(t) \Rightarrow S(R) = GI_{ubph}(R) + S_0, \ R = ct/2 \qquad (1)$$

where G is the total electronic gain, $I_{ubph}(R) = \xi_{ph} P_r(R)$ is the unbiased photodetector current (ξ_{ph} is the photodetector responsivity and P_r is the retroreflected radiation power) and S_0 is the background component, accumulating all types of electric displacement and low-frequency noise that can be assumed to be constant during the relatively short measurement time: about 67 μs for a range of 10 km, according to relation (1).

A theoretical estimation of P_r is given by the lidar equation:

$$P_r(R) = E_l \frac{c\beta(R)}{2} \frac{A_{rec}}{R^2} \tau_{tr}\tau_{rec} \exp\left(-2\int_0^R \alpha(R')dR'\right) \ (2)$$

where E_l is the output laser pulse energy, β the backscattering coefficient of the medium, A_{rec} the effective receiver area, τ_{tr} and τ_{rec} the transmitter and receiver efficiencies, and α the extinction coefficient.

At the early stage of a fire, the characteristic spread of the smoke plume in the direction of laser-beam propagation ΔR_{sp} (Fig. 2) is about 10 m. To be able to reveal specific few-meter scale structures that make the smoke-plume signatures different from other lidar returns, the data-acquisition unit must measure the photodetector output with a sampling interval $\delta R \sim 1.5$ m, eventually yielding

the discrete-time lidar signal in the form

$$S(R(t)) = C_0 \frac{\beta(R)}{R^2}\exp\left(-2\int_0^R \alpha(R')dR'\right) + S_0,$$

$$C_0 = G\xi_{ph}E_l\frac{c}{2}A_{rec}\tau_{tr}\tau_{rec} = const, \qquad (3)$$

digitized at the points $t_i = 2R_i/c$, $R_i = i\,\delta R$, $i = 0,1,\ldots,i_{max}$, $i_{max} = R_{max}/\delta R$.
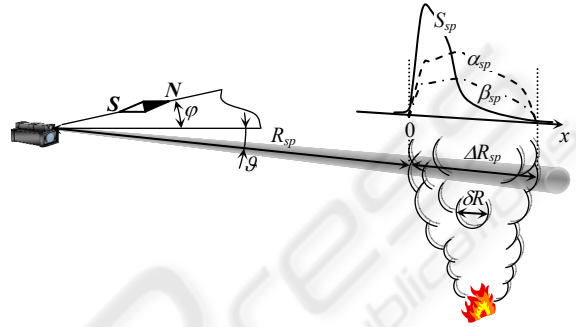

Figure 2: The main spatial parameters of smoke-plume detection.

According to (1) and (2), smoke plumes manifest themselves in raw lidar signals as peaks whose amplitude and shape vary due to the stochastic changes in the particle distribution within the smoke plume under the action of gas-dynamic forces, buoyancy and wind. The smoke-plume signatures are observed against a background contaminated by electronic and atmospheric noise (Fig. 3). Electronic noise of a well constructed receiver usually demonstrates no dependence on the distance and can be estimated from a signal segment recorded far beyond the range of the instrument, where no signal attributable to retroreflection is expected.
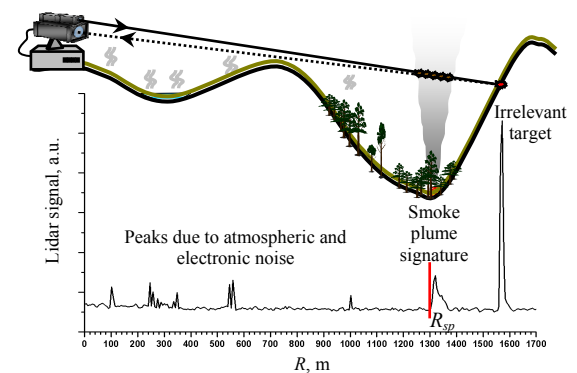

Figure 3: Composition of the raw lidar signal.

Apart from this unstructured noise, the lidar signal may contain peaks due to retroreflection from hills, trees, buildings, birds, etc. Solid-target signatures

are narrow pulse-like waveforms, since the backscattering occurs at almost a single distance. The shape of these peaks is mainly defined by the bandwidth of the detection channel and the rate of the analog-to-digital conversion.

3 RECOGNITION STRATEGY

3.1 Characterization

As seen from (3), the shape of the smoke-plume signatures in the lidar signal depends in a complicated way on the profiles of the extinction and backscattering coefficients along the beam propagation direction. Although important for prediction of the lidar range, gas-dynamic smoke-plume models do not provide a solid basis for the extraction of the characteristic features of the smoke-plume signature. Due to this lack of reliable parametric models, automated fire surveillance is mainly based on artificial-intelligence algorithms such as neural network (NN) methods.

In principle, lidar identifies targets with the precision of a few meters, thus allowing for a very accurate location of the fire. The angular target position (the azimuth φ and elevation ϑ, see Fig. 2) is given by the laser beam direction, but the calculation of the distance to the smoke plume R_{sp} is carried out by the signal analysis unit.

NN architectures and algorithms suited for lidar data extraction have been discussed in the literature since the 1990s (Bhattacharya et al., 1997). It was established that waveforms containing small retroreflection from distributed targets could not be directly presented to a neural network. A simple and fast preprocessing method was developed for facilitating the recognition, ensuring, at the same time, that the processed waveforms properly reflect subtle variations in the original waveforms. Following the same principles as the radial-basis function algorithms (Bishop, 1995; Haykin, 1999), the recognition efficiency of a perceptron-based NN is enhanced by a special binarization procedure that uses a 2D grid in the signal-distance plane for the waveform representation and a point-to-node proximity criterion for assigning one or zero to the grid nodes. Each node is treated as a separate input component, increasing the network input dimension, number of adjustable weights and, according to Cover's theorem (Haykin, 1999), improving pattern separability.

3.2 Problems

The application in question is characterized by the following difficulties:

1. The length of the discrete-time sequence to be processed, $i_{\max} = R_{\max} / \delta R \sim 6.7 \times 10^3$, is much larger than in other lidar applications, such as underwater object detection (Mitra et al., 2003). As a result, the conventional NN algorithms (Bhattacharya et al., 1997; Mitra et al., 2003) cannot be straightforwardly applied because they require excessive computation time and resources. In addition, fire may occur anywhere within the surveillance range, so no narrower region of interest can be selected a priori.

2. Smoke-plume signatures are compact. As seen from Eq. (3), for a starting fire the characteristic spread of a smoke-plume signature ΔR_{ss}, within which the backscattering factor β is sufficiently large to produce the signal above the noise level, is restricted by the spread of the plume: $\Delta R_{ss} \leq \Delta R_{sp} \approx 10$ m. Well-developed fires result in much wider plumes, but denser smoke increases the laser-beam extinction up to the values $\alpha \sim 0.2$ m^{-1} (Kozlov and Panchenko, 1996). In these circumstances, the smoke-plume signature decreases down to the noise level at distances of the order of α^{-1} due to the Beer-Lambert absorption of both the laser beam and retroreflected light, resulting in $\Delta R_{ss} \sim 5$ m. Measured as number of points in the digitized signal, $N_{ss} = \Delta R_{ss} / \delta R$, the signature spread is always much less than that for the cases described by Bhattacharya et al. (1997) and Mitra et al. (2003), typically consisting of 5-10 points. The short signature width and the great variety of possible waveforms impede application of statistics-based algorithms for noise reduction and signal compression, which effectively reduce the computational load in many other applications (Mitra et al., 2003).

3. The fact that the distance to the target R_{sp} must be determined during the recognition may complicate the NN structure: for the straightforward algorithms, it turns the multiple input - single output classification scheme into one with multiple outputs, in which the additional neurons codify, in an analog or digital way, the value of $R_{sp.}$

4. Due to the fact that a constant background can be represented as a sum of uniformly distributed peaks, the problem of peak recognition is not linearly separable a priory and cannot be solved without introduction of preprocessing and/or non-linearity.

3.3 Knowledge and Invariances

According to general indications (Anderson, 1988), to solve the problems presented in Sec. 3.2, a specialized NN algorithm must be developed, incorporating all prior information in order to simplify the overall structure and facilitate the recognition. Depending on its nature, the knowledge about the input signal can be represented as a transformation, selection rule and/or invariant and then built into the system via specific design or preprocessing procedures (Haykin, 1999).

The analysis of the lidar signal, briefly presented in subsections 2.1, 2.2 and 3.2, makes it possible to point out the following peculiarities:

1. The smoke-plume signatures manifest themselves in the raw lidar signal as peaks whose characteristic width ΔR_{ss} (several meters) is much less than the typical distance to the smoke plume R_{sp} (from hundred meters to several kilometers).

2. The position of the smoke-signature maximum corresponds to the desired distance to the smoke plume.

3. The local noise level may be estimated as the root-mean-square of the signal just before and after the peak and the segment of the lidar signal of the length $\sim 3\Delta R_{ss}$, containing the smoke-signature maximum in its center, is supposed to provide information of both the smoke-signature shape and the local noise. The ratio of the peak amplitude to the mean local noise, called peak-to-noise ratio (*PNR*), represents an important scale-independent characteristic of the peak magnitude, closely linked with the probability of the peak to be a target signature rather than clutter. For this reason, it is worthwhile to treat *PNR* as an invariant characteristic feature to be extracted and presented for recognition in a separate way.

Within the range $10\Delta R_{ss} \leq R \leq R_{max}$ the shape factor of the smoke-plume signature is invariant with respect to the distance R (Utkin et al., 2009). Obviously, the noise distorts the smoke-plume signatures more at greater distances, and the pattern-recognition problem in question can be treated as distance-independent in the sense that the recognition conditions for a tenuous smoke plume are equivalent to those for a dense plume observed at a greater distance provided that the signal-to-noise ratio is the same.

3.4 Implementation

The knowledge and invariances are built into the system via the following preprocessing procedure:

The raw lidar signal consisting of several thousand points ($i_{max} = R_{max} / \delta R$) is viewed by the preprocessing software through a window of several tens of points ($\sim 3\Delta R_{ss} / \delta R$) that moves along the signal curve. The window motion stops if the local signal maximum coincides with the window center R_w and the corresponding peak-to-noise ratio $PNR(R_w)$ is calculated. If $PNR(R_w) < PNR_{thr}$, where the threshold value PNR_{thr} (typically, from 3 to 5) is chosen in accordance with the sensitivity of a given lidar system, the peak is considered to be too small for being a smoke-plume signature and the observation window continues its motion along the lidar-signal curve. Otherwise the signal pattern within the window is sent to the recognition unit. The corresponding feature value $PNR(R_w)$ is introduced directly to the NN through a special input (Fig. 4).

Eventual alarm generation is performed on the basis of pattern classification (smoke-signature dichotomy) with a single-layer neural network (perceptron), which is functionally equivalent to the adaptive linear filter (Haykin, 1999).
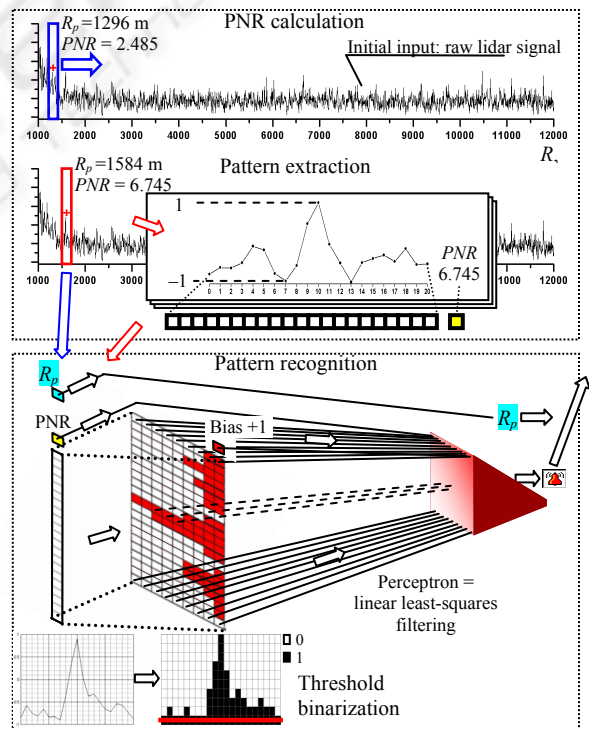

Figure 4: Stages of the smoke-signature recognition procedure.

Borrowing the approach from the radial-basis function network theory (notably, it can be shown that the binarization processing correspond to a radial-basis function technique with some specific norm), classification efficiency of the perceptron is enhanced by nonlinear *threshold binarization* transformation to higher dimensional space, similar to Bhattacharya's processing of lidar signal (Bhattacharya et al., 1997) for the detection of fish in near-shore waters: The signal pattern is mapped on a rectangular 2D grid. Each sample point is checked against the grid-crossing points. If a sample point falls within half a grid space on either side in both the horizontal and vertical directions, a one is assigned at that point; otherwise, a zero is assigned. Each sample point is tested in the same way, yielding at the end a matrix of zeros and ones, eventually converted into a longer binary pattern vector reflecting all the peculiarities of the pattern, provided that a sufficiently fine grid is chosen.

When the vertical grid spacing equals the lidar sampling distance so that all the signal points are located on the vertical grid lines, the above algorithm reduces to a simple *point binarization* of the signal with resolution corresponding to the horizontal grid spacing. The *threshold binarization* procedure, corresponding to the point binarization in which a one is assigned to each grid point situated below any point already assigned to one, is even easier for hardware implementation (a batch of threshold detectors with linearly increasing thresholds) and results in less sparse and more compact binarized samples: the bottom line always contains ones and can be discarded.

Notably, the number of binarization levels is a free parameter of the recognition scheme. Decreasing the number of levels, one can produce rougher binary signal description and, at the same time, reduce the signal dimension and the number of adaptive parameters of the recognition process. Being chosen on the basis of the bias-variance trade-off (Haykin, 1999), the number of binarization levels plays the same role as the number of training epochs in the iterative learning rules.

The *supervised learning procedure* is implemented through the least-squares filtering. For a given training set, it readily yields a unique deterministic solution (Haykin, 1999) for the desired interconnection weights as a product of pseudoinverse of the matrix composed from the binarized training samples and the vector of corresponding classification tags (here, 1 for the smoke-signature peaks and −1 for the spurious signal peaks).

Following Bishop's recommendations (Bishop, 1995), the instability arisen from the sparse nature of the binary-sample matrices and incomplete ranks is overcome by stabilized pseudoinversion on the basis of singular-value decomposition (Press et al., 1986). The binary input has two additional entries: one for the constant activation bias (+1) and the other for the *PNR* value that passes to the perceptron without binarization. The alarm signal is accompanied by the current position of the moving window center $R_w \approx R_{sp}$ that corresponds to the maximum of the retroreflected radiation and thus provides the desired distance to detected smoke plume.
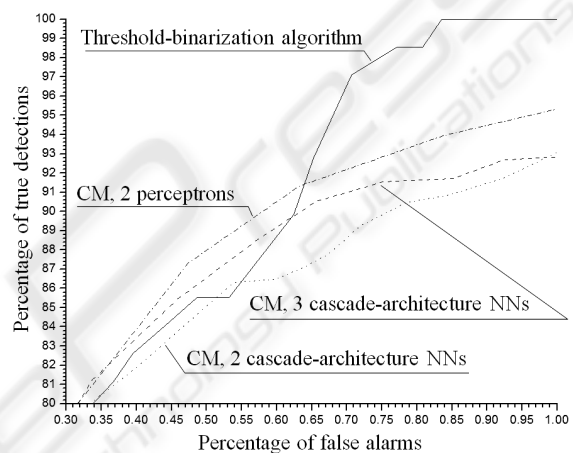

Figure 5: ROC curves corresponding to the developed threshold-binarization algorithm and the three committee machines described by Fernandes et al. (2004).

4 RESULTS

Fig. 5 illustrates comparison of the developed threshold-binarization algorithm with three more complicated artificial-intelligence methods developed for smoke-signature recognition in the lidar signal (Fernandes et al., 2004). The threshold-binarization algorithm demonstrated superior efficiency in the area of false alarm rate greater than 0.65%, resulting to 100% detection of the smoke signatures in the validation set at the false alarm rate as low as 0.84% (91 false detections at recognition of 10891 noise peaks in 112 recorded lidar signals).

At the same time, the proposed algorithm:
- yields nearly one order of magnitude faster training;
- the developed supervised learning procedure is not connected with the choice of the best classifier, so it can be strictly formalized and performed by users without special instruction;

- the learning procedure is fast and of predictable duration: it does not involve repetitive/iterative routines like training epochs in the case of gradient-descent methods and
- the global minimum of the classification error for given training set is readily achieved by a sequence of matrix operations of guaranteed stability.

At very close distances to the lidar, $R \leq 10\Delta R_{ss}$, the shape factor of the smoke-plume signature does depend on R_{sp}. However, it was observed that the shape distortion does not affect the recognition capability of the system for this region, mostly due to very high *PNR* feature value that activates the alarm output even if the input from the binary-sample nodes is not univocal.

5 CONCLUSIONS AND FUTURE WORK

The neural-network algorithm in question is extremely flexible; it was successfully used for automated signal processing in a variety of lidars, including a system for forest fire surveillance already deployed in Central Portugal within the framework of the AGRO project supported by Portuguese Ministry of Agriculture.

As compared to alternative methods of automated fire detection, which mostly focus on radiometry and video/infrared imaging (San-Miguel-Ayanz et al., 2005), the present active technique, due to its potentially higher sensitivity, offers quicker response to the alarm situation. In addition, automation of the 1D lidar signal processing is an easier task than fire or smoke-plume recognition in the 2D images provided by video/infrared cameras.

Future developments of the described algorithm are connected with invoking additional information extracted from statistical properties of the collected lidar returns.

ACKNOWLEDGEMENTS

REFERENCES

Anderson, J.A., 1988. General Introduction. In.: *Anderson, J.A., Rosenfeld, E. (eds.): Neurocomputing: Foundations of Research,* MIT Press. Cambridge.

Bhattacharya, D., Pillai, S.R., Antoniou, A., 1997. Waveform classification and information extraction from lidar data by neural networks. *IEEE Trans. on Geoscience and Remote Sensing* 35, 699-707.

Bishop, C.M., 1995. *Neural Networks for Pattern Recognition*, Claredon Press. Oxford.

Fernandes, A.M., Utkin, A.B., Lavrov, A.V., Vilar, R.M., 2004. Development of neural network committee machines for automatic forest fire detection using lidar. *Pattern Recognition* 37, 2039-2047.

Haykin, S., 1999. Neural Networks, Prentice Hall. London, 2nd edition.

Kozlov, V.S., Panchenko, M.V., 1996. Investigation of optical characteristics and particle-size distribution of wood-smoke aerosols. *Combustion, Explosion, and Shock Waves* 32, 577-586.

Mitra, V., Wang, C.J., Banerjee, S., 2003. Lidar detection of underwater objects using neural networks with linear prediction and fourier transform for feature extraction. In *Proceedings of Application of Neural Networks in Engineering, ANNIE'2003*, Vol. 13. ASME Press. Missouri, 695-700.

Press, W.H., Flannerly, B.P., Teukolsky, S.A., Vetterling W.T., 1986. *Numerical Recipes: The Art of Scientific Computing*, Cambridge Univ. Press. Cambridge.

San-Miguel-Ayanz, J., Ravail, N., Kelha, V., Ollero, A., 2005. Active fire detection for fire emergency management: Potential and limitations for the operational use of remote sensing. *Natural Hazards* 35, 361-376.

Utkin, A.B., Lavrov, A.V., Vilar, R.M., 2009. Low-cost active optical system for fire surveillance. *Optics and Spectroscopy* 106, 926-936.